

# IL NUOVO CIMENTO

ORGANO DELLA SOCIETÀ ITALIANA DI FISICA  
SOTTO GLI AUSPICI DEL CONSIGLIO NAZIONALE DELLE RICERCHE  
E DEL COMITATO NAZIONALE PER L'ENERGIA NUCLEARE

VOL. XXIII, N. 1

*Serie decima*

1° Gennaio 1962

## Interactions of $\pi^-$ -Mesons of Kinetic Energy 915 MeV with Carbon Nuclei.

N. ABBATTISTA, M. BIASCO, S. MONGELLI, A. ROMANO and P. WALOSCHEK (\*)

*Istituto di Fisica dell'Università - Bari*

E. PEREZ-FERREIRA

*Comisión Nacional de Energía Atómica - Buenos Aires*

(ricevuto il 29 Luglio 1961)

**Summary.** — Interactions of  $\pi^-$  mesons with carbon nuclei were studied with a propane bubble chamber. The total cross-section on carbon was found to be  $(383 \pm 20)$  mb of which  $(89 \pm 12)$  mb corresponded to elastic scattering. A detailed description of the events with re-emission of a  $\pi^-$  is made. The diffraction scattering angular distribution and the total cross section obtained were described by an optical model using an imaginary gaussian potential. The r.m.s. radius of this potential obtained was  $3.0 \cdot 10^{-13}$  cm, which is considerably greater than the corresponding radius obtained for the electric charge distribution.

### 1. — Introduction.

Interactions of fast pions with nuclei may provide valuable information on nuclear structure and on some aspects of pion-nucleon interaction which are difficult to analyse with free protons. In the present paper we report results obtained from interactions of  $\pi^-$ -mesons with C nuclei in a propane bubble chamber (\*\*).

(\*) On leave of absence from Istituto Nazionale di Fisica Nucleare - Sezione di Bologna.

(\*\*) We are very grateful to the bubble chamber group of the Columbia University and in particular to Prof. J. STEINBERGER for allowing us to perform these measurements on films obtained at the Brookhaven Cosmotron.

After a description of the experimental results (Section 2), we discuss the inelastic re-emission processes and finally the results on the size of the carbon nucleus obtained from an analysis of the diffraction scattering pattern. We compare our results with measurements on helium and hydrogen at different energies. We observe a difference in the apparent r.m.s. radius of the carbon nucleus for its interactions with  $\pi^-$ -mesons of 915 MeV, to that obtained from the analysis of electron scattering measurements. This may be explained as an effect of the 890 MeV  $\pi^- + p$  resonance or by means of a different distribution of protons and neutrons in the carbon nucleus. Both hypotheses are discussed in Section 4.

## 2. - Experimental part.

2.1. - A total number of 4355 events was found during the scanning of 5.38 km of  $\pi^-$ -meson tracks in the 12 in. propane bubble chamber. The beam energy was  $(915 \pm 25)$  MeV as it was discussed in ref. (1) where further references on previous works with the same beam can be found.

The prong distribution for carbon interactions was obtained from our propane data by subtracting the contribution expected from hydrogen. Data from Saclay (2) and Bologna (3) obtained with hydrogen target and bubble chambers were used. Table I summarizes the classification of the observed events and the estimated number of collisions on hydrogen.

All events were analyzed following the graphical method (4) which was somewhat modified in order to perform nearly all computations on an electronic computer (\*).

For those events in which a single  $\pi^-$ -meson emerged, we determined its momentum and angle with respect to the incident particle. In order to reduce errors, only those events which occurred in a fiducial region were accepted;

(1) S. BERGIA, L. BERTOCCHI, V. BORELLI, G. BRAUTTI, L. CHERSOVANI, L. LAVATELLI, A. MINGUZZI-RANZI, R. TOSI, P. WALOSCHEK and V. ZOBOLI: *Nuovo Cimento*, **15**, 551 (1960).

(2) J. C. BRISSON, G. DETOEF, P. FALK-VAIRANT, L. VAN ROSSUM, G. VALLADAS and L. C. L. YUAN: *Phys. Rev. Lett.*, **3**, 561 (1959).

(3) V. ALLES-BORELLI, S. BERGIA, E. PEREZ-FERREIRA and P. WALOSCHEK: *Nuovo Cimento*, **14**, 211 (1959); V. BORELLI, A. MINGUZZI-RANZI, P. WALOSCHEK and V. ZOBOLI: *Suppl. Nuovo Cimento*, **11**, 447 (1959).

(4) V. BORELLI, P. FRANZINI, I. MANNELLI, A. MINGUZZI-RANZI, R. SANTANGELO, F. SAPORETTI, V. SILVESTRINI, P. WALOSCHEK and V. ZOBOLI: *Nuovo Cimento*, **15**, 525 (1958).

(\*) The computations were performed at the IBM 650 of the Centro Calcoli of the University of Bologna. We are grateful to the Centro Calcoli Group.

we also excluded those individual events clearly identified as  $\pi^- + p$  elastic scatterings from measurements already made by the Bologna group (1).

TABLE I.

		Number of positive prongs							Totals
		0	1	2	3	4	5	6	
Number of negative prongs	0	177 (+212 H)	226	184	87	22	4	1	701 (+212 H)
	1	893	784 (+926 H)	389	140	49	8	3	2266 (+926 H)
	2	11	39	62 (+9 H)	25	12	2	—	151 (+9 H)
	3	2	2	3	—	1	—	—	8
								3126 (+1147 H)	
Unclassified events								82	
Total								4355	

2.2. *Diffraction scattering.* — The momentum spectrum of events in which only a single  $\pi^-$ -meson emerged without any other prongs, is shown in Fig. 1; it presents a very pronounced peak around 1000 MeV/c particularly for events of scattering angle smaller than  $14^\circ$ .

This peak should contain diffraction scattering events on carbon together with several contaminations that could not be separated by our momentum measurements.

A particular study was made on events which could be collisions with bound nucleons which we call « pseudoelastic ». Events of this type were found inside a compatibility region given by the kine-

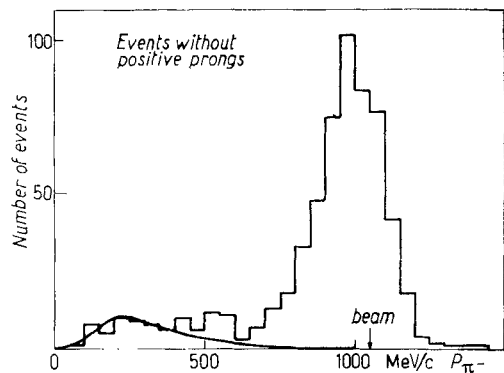


Fig. 1. --  $\pi^-$  momentum spectrum of events with no other prongs. The curve corresponds to the  $\pi^-$  spectrum expected from  $\pi$  production events on  $H_2$ .

matics of the scattering on a moving nucleon. For large scattering angles the results were compatible with the cross-sections on free nucleons, but at small angles (particularly for the  $\pi^- + p_c$  case) the number of events was decreasing rapidly. This effect is certainly due to the Pauli principle which forbids collisions with small momentum transfer.

As a result of this analysis we deduced that at angles smaller than  $14^\circ$  very few  $\pi^- + n_c$  events should be present in our apparently elastic peak and that the possible small contamination would in every case be limited to the interval  $9^\circ \div 14^\circ$ .

Nothing can be said about events in which the carbon remains excited ( $(20 \div 30)$  MeV) and about any type of (real) potential scattering contaminating our diffraction peak. The only argument is *a posteriori* and comes from the optical model calculations presented in Section 3: if such contributions are present the remaining amount of diffraction scattering would be incompatible with the high total cross-section observed, at least as long as we use reasonable radii for the absorbing potential ( $R < 5 \cdot 10^{-13}$  cm).

The measured peak for the secondary  $\pi^-$ -mesons of 1000 MeV/c (shown in Fig. 1) differs by 50 MeV/c from the incident momentum ( $1050 \pm 25$ ) MeV/c (\*). This difference may be explained as the result of the inclusion of some inelastic events, but we cannot exclude the possibility of systematic errors of measurement making some contribution.

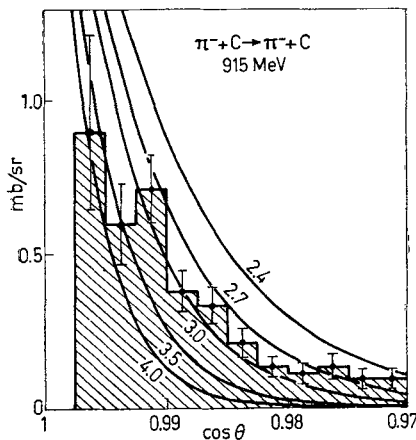


Fig. 2. — Angular distribution for events classified as elastic on carbon. The curves represent the diffraction from a gaussian imaginary potential with different values of the r.m.s. radius.

For different intervals of the scattering angle, azimuth plots were made in order to determine our scanning efficiency. A correction for scanning losses was calculated and applied to the data for  $\theta \geq 4^\circ$  (see Table II). For  $0^\circ < \theta < 4^\circ$  the scanning efficiency was found to be too low and the corresponding contribution was interpolated using the  $0^\circ$  value obtained from the optical theorem neglecting the contribution to the scattering cross-section from the real part of the amplitude. The final figure for the corrected number of elastic scatterings ( $< 14^\circ$ ) was 867 events; this corresponds to an «elastic» scattering cross-section

$$\sigma_{el} = (89 \pm 12) \text{ mb} .$$

(\*) As determined by analysis of the reactions  $\pi^- + p \rightarrow \Lambda^0 + \theta^0$  observed in the same film by F. EISLER *et al.*: *Nuovo Cimento*, **7**, 222 (1958).

The error was obtained after considering statistical fluctuations and uncertainties on all corrections applied, particularly the unknown contribution of events of more than  $14^\circ$ .

In Table II is presented the angular distribution from all events with measured momentum of more than 700 MeV/c. Fig. 2 shows the corresponding histogram.

TABLE II.

cos scattering angle interval	Real no. of events	Corrected no. of events
0.9975 $\div$ 0.9950	68	136
0.9950 $\div$ 0.9925	55	92
0.9925 $\div$ 0.9900	70	109
0.9900 $\div$ 0.9875	39	57
0.9875 $\div$ 0.9850	36	51
0.9850 $\div$ 0.9825	24	33
0.9825 $\div$ 0.9800	14	20
0.9800 $\div$ 0.9775	13	18
0.9775 $\div$ 0.9750	15	21
0.9750 $\div$ 0.9725	10	14
0.9725 $\div$ 0.9700	10	14

2'3. *Inelastic events.* — As is shown in Table I we observed 3126 interactions with carbon nuclei. Of these 450 were classified as elastic scattering. The remainder correspond to a cross-section

$$\sigma_{in} = (294 \pm 18) \text{ mb}.$$

In 39% of the inelastic events a  $\pi^-$ -meson emerges. We have measured the emission angle and momentum of events of this type. The results are

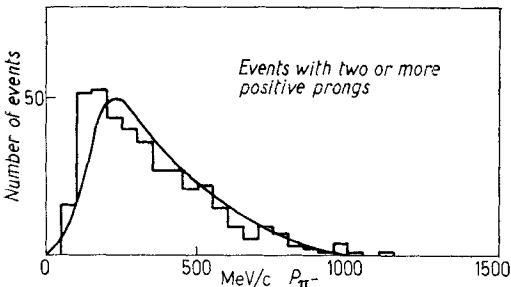


Fig. 3a. —  $\pi^-$  momentum spectrum of events with two or more positive prongs. The curve corresponds to the pion spectrum expected from  $\pi^-$  production events on  $H_2$ .

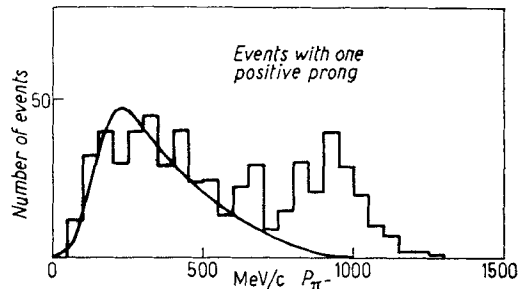


Fig. 3b. —  $\pi^-$  momentum spectrum of events with one positive track, corrected for  $H_2$  contamination. The curve corresponds to the pion spectrum expected from  $\pi^-$  production events on  $H_2$ .

shown in Fig. 3 and 4. The momentum distribution was obtained from the observed « propane »-spectra, after subtracting the contribution of two prong events expected from hydrogen. The hydrogen spectra used were obtained from the data of the Bologna group observed at 960 MeV in a hydrogen bubble chamber (<sup>2</sup>). For comparison the hydrogen spectra are included in Fig. 3 in

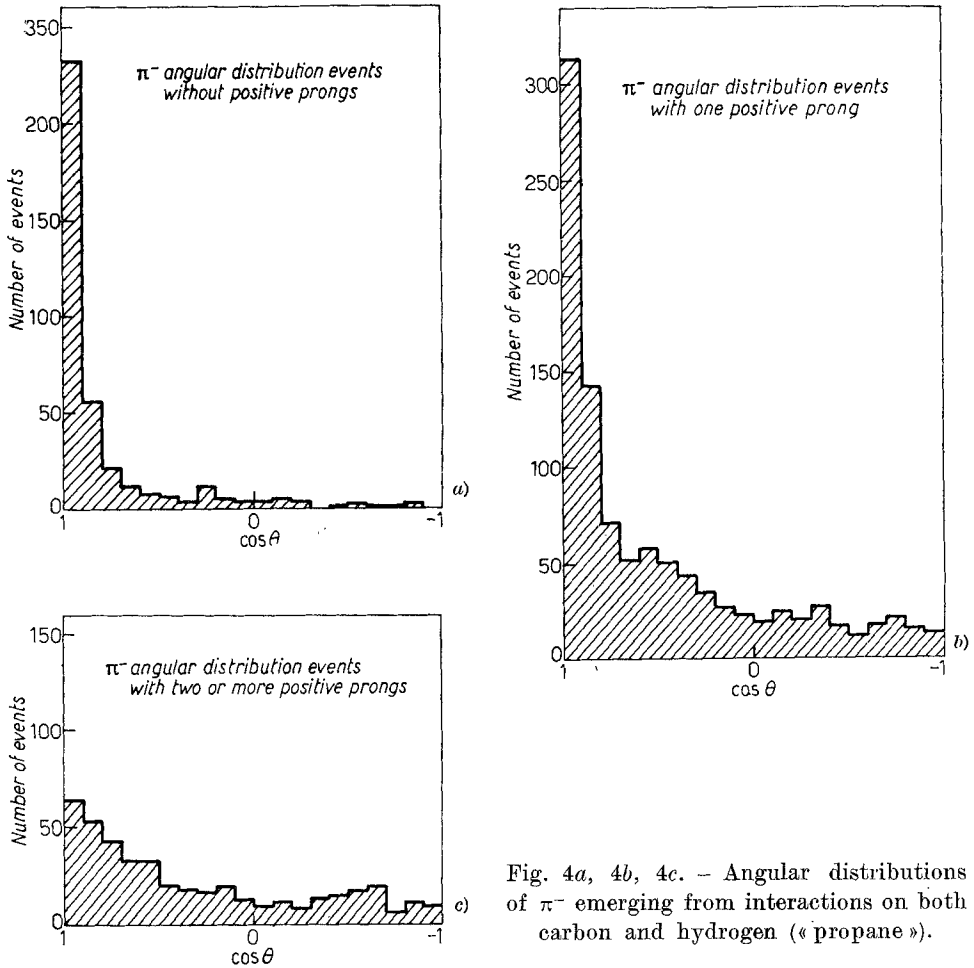


Fig. 4a, 4b, 4c. — Angular distributions of  $\pi^-$  emerging from interactions on both carbon and hydrogen (« propane »).

form of smoothed curves. The hydrogen events are all pion production events and the similarity of the hydrogen and carbon spectra suggests that in carbon also, these events are mainly due to pion production. In Fig. 3b a number of events around 900 MeV/c are of the « pseudoelastic » type discussed in Section 2'2.

### 3. - Optical model parameters.

The total cross-section and the diffraction scattering angular distribution may be calculated by means of an optical model. From this point of view the carbon nucleus is quite opaque and the high absorption can be represented by an imaginary potential. For light nuclei the form of this potential is conveniently assumed to be gaussian (or similar) as has been shown in electron scattering experiments <sup>(5)</sup>. We have tried to fit our experimental data with a model in which the nuclear potential is assumed to have a gaussian form; we have neglected the very small Coulomb scattering contribution. The angular distributions were obtained in Born approximation. Since the potential used must explain the strong absorption cross-section observed we assume it as being purely imaginary. This exceeds the usual interpretation of the Born approximation but the formulas obtained here are equally valid as it has been shown by BELENKY <sup>(6)</sup>. The experimental elastic scattering differential cross-section is roughly fitted using a relatively large value for the nuclear radius. The inclusion of any real potential would force us to use even higher radii for the imaginary part. This reason induced us to assume as negligible the real part of the nuclear potential.

For a potential of the form

$$(1) \quad U = U_0 \exp \left[ -\frac{3}{2} \left( \frac{r}{a} \right)^2 \right],$$

where  $a$  represents the r.m.s. radius defined by

$$(2) \quad a^2 = \int_0^{\infty} 4\pi r^2 \cdot r^2 \cdot \rho(r) dr,$$

$$(3) \quad 1 = \int_0^{\infty} 4\pi r^2 \cdot \rho(r) dr,$$

( $\rho(r)$  is a density distribution) the angular distribution calculated in the Born approximation is:

$$(4) \quad \frac{d\sigma}{d\Omega} = \frac{\mu^2 \pi |U_0|^2}{4 \cdot \left(\frac{3}{2} (1/a^2)\right)^3} \cdot \exp \left[ -\frac{4}{3} \left( \frac{a}{\lambda} \right)^2 \sin^2 \frac{\theta}{2} \right], \quad (\hbar = c = 1),$$

( $\mu$  = reduced mass).

<sup>(5)</sup> R. HOFSTADTER: *Rev. Mod. Phys.*, **28**, 214 (1956).

<sup>(6)</sup> S. Z. BELENKY: *Sov. Phys. JETP*, **3**, 813 (1956).

For a purely imaginary potential, the scattering amplitude is also imaginary, and we can apply the optical theorem for the forwards amplitude:

$$(5) \quad \left(\frac{d\sigma}{d\Omega}\right)_0 = \left(\frac{\sigma_{\text{tot}}}{4\pi\lambda}\right)^2 = \frac{\pi\mu^2 |U_0|^2}{4 \cdot \left(\frac{3}{2}(1/a^2)\right)^3}.$$

Consequently for known  $\sigma_{\text{tot}}$ ,  $U_0$  may be expressed as a function of  $a$  and  $(d\sigma/d\Omega)_0$ . There is only one free parameter.

Fig. 2 shows a set of curves obtained with formula (4) for different values of these parameters. We estimate as reasonable the curve for

$$a = 3.0 \cdot 10^{-13} \text{ cm}$$

and  $U_0 = i \cdot 365 \text{ MeV}$ ; the error must take into account the uncertainties of the small angle corrections, the not particularly well fitting data as well as the eventual inelastic contamination and may be estimated as  $\begin{smallmatrix} +0.30 \\ -0.20 \end{smallmatrix}$ .

The high value of the imaginary potential is well explained by the high  $\pi^- + p$  cross-section near 900 MeV. One can relate the mean  $\pi^-$ -nucleon cross-section  $\bar{\sigma}$  with the imaginary potential through the relation (?)

$$(6) \quad U_{\text{im}} = \frac{1}{2\lambda m} \bar{\sigma} \rho,$$

where  $\rho$  is the density of nucleons.  $\rho$  can be estimated for the central region of the carbon nucleus from the Hofstadter experiments as twice the proton charge density,  $\rho \approx 0.16$  nucleons/fermi<sup>3</sup>. With  $\bar{\sigma} = 35 \text{ mb}$  (where some allowance was made for the Pauli principle) we find  $U_0 \approx i \cdot 400 \text{ MeV}$ . Naturally this is only a very rough check because the central values of both the nucleon density and the potential are very insensitive to our experimental measurements. For the carbon nucleus this is made evident in the Born approximation, where the integral  $\int 4\pi r^2 U(r) dr$  (which gives the angular distribution) is nearly independent of the values of  $U(r)$  for  $r < 1.5$  fermi.

The r.m.s. is, instead, a parameter better defined by scattering experiments. The radius obtained for carbon in electron experiments is  $a = (2.40 \pm 0.05) \cdot 10^{-13} \text{ cm}$  which may be compared with our value of  $3.0 \cdot 10^{-13} \text{ cm}$ .

#### 4. - Comparison with other experiments and discussion.

There are experiments performed with pions on helium and hydrogen from which the r.m.s. radii of these nuclei can be deduced. The helium data obtained

---

(?) P. MITTELSTAEDT: *Zeits. Naturfor.*, **12a**, 947 (1957).

by the Trieste group <sup>(8)</sup> give the following r.m.s. radii (\*):

$$a = 1.78 \cdot 10^{-13} \text{ cm} \quad \text{at} \quad 970 \text{ MeV}$$

$$a = 1.60 \cdot 10^{-13} \text{ cm} \quad \text{at} \quad 1670 \text{ MeV}$$

while the corresponding r.m.s. radius with electrons is

$$a_0 = 1.61 \cdot 10^{-13} \text{ cm}.$$

The value at 970 MeV differs from the electromagnetic radius, but not so drastically as the carbon radius at 915 MeV.

If we interpret the larger r.m.s. radii as an effect of the pion cloud, particularly strong near the  $\pi^- + p$  resonances, we may also observe this effect in pion-proton scattering. But here the interference effects can mask completely the diffraction pattern; the radii obtained from the experiment must be taken with reserve (\*\*). In order to make the model and definition of radii uniform, we reanalysed the pion-proton data from 915 <sup>(4)</sup>, 1200 <sup>(9)</sup>, and

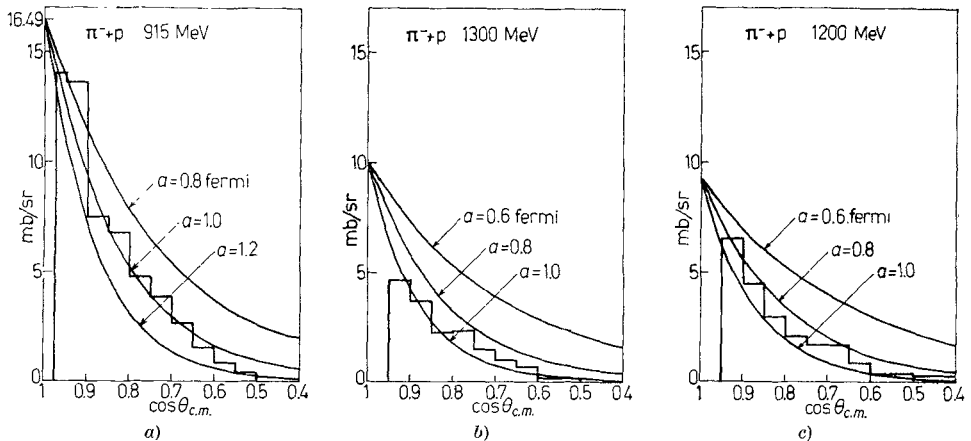


Fig. 5a, 5b, 5c. - Angular distributions for  $\pi^- + p$  elastic scattering compared with curves for different r.m.s.-radii of an imaginary gaussian potential.

<sup>(8)</sup> G. BRAUTTI, L. CHERSOVANI, C. FRANZINETTI, M. SEDMAK-FURLAN and R. TOSI-TORELLI: *Nuovo Cimento*, **19**, 1270 (1961).

(\*) The r.m.s. radius is related to the radii given by BRAUTTI *et al.* <sup>(8)</sup> through the formula  $R = \sqrt{\frac{2}{3}} a$ .

(\*\*) On carbon the elastic scattering is reduced to a small forwards peak and therefore we assume that resonant or potential scattering is not important.

<sup>(9)</sup> L. BERTANZA, R. CARRARA, A. DRAGO, P. FRANZINI, I. MANNELLI, G. V. SILVESTRINI and P. H. STOKER: *Nuovo Cimento*, **19**, 467 (1961).

1300 MeV <sup>(10)</sup> (shown in Fig. 5), obtaining the following results:

$$a = 1.0 \cdot 10^{-13} \text{ cm } (*) \quad \text{at } 915 \text{ MeV}$$

$$a = 0.90 \cdot 10^{-13} \text{ cm} \quad \text{at } 1200 \text{ MeV}$$

$$a = 0.95 \cdot 10^{-13} \text{ cm} \quad \text{at } 1300 \text{ MeV}.$$

While at 1200 and 1300 MeV the radii are probably well defined (small resonance scattering), at 915 MeV it is hard to define a diffraction peak. Under the assumption that diffraction and resonance scattering are not interfering destructively we may say that the given radius represents a lower limit.

New experiments may increase our knowledge about the nuclear radii, and particularly clarify if there is an energy dependence in the resonance region.

If this should be the case one could draw some conclusion about a higher opacity of the meson cloud. Experiments with helium and propane bubble chambers are particularly indicated for this purpose.

Another hypothesis which could explain the large carbon radius could be the assumption of a different distribution of neutrons and protons inside the nucleus. In order to explain our experimental results, neutrons and protons should be distributed radially in the manner shown in Fig. 6. The proton distribution was taken equal to the electric charge distribution, and relation (6) was used

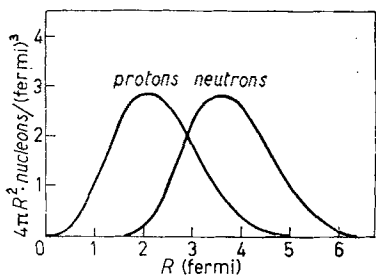


Fig. 6. - Radial distribution of protons and neutrons in the carbon nucleus which would explain the different carbon radius observed with pions and electrons.

to add the absorption power of protons and neutrons.

The last hypothesis could be checked in a  $\pi^+$ +carbon experiment at  $\sim 900$  MeV. The high  $\pi^+$ +n cross-section should make the carbon nucleus appear even bigger. The r.m.s. radius expected in the proposed experiment is  $\sim 4 \cdot 10^{-13}$  cm.

\* \* \*

We are very grateful to Profs. M. MERLIN and G. PUPPI for their continuous encouragements and assistance.

(\*) These values were obtained by trying to fit the distributions up to  $\cos \theta \approx 0.5$ . Errors may be estimated from the shown figures.

<sup>(10)</sup> M. CHRETIEN, J. LEITNER, N. P. SAMIOS, M. SCHWARTZ and J. STEINBERGER: *Phys. Rev.*, **108**, 383 (1957).

Many helpful discussions with Drs. G. COSTA and L. TENAGLIA clarified the interpretative aspects of the work.

The work was carried out with financial help from the N.A.T.O. Research Grants Programme and from the Istituto Nazionale di Fisica Nucleare; for their assistance we are very grateful.

## APPENDIX I

### The $\pi^-+p$ elastic scattering cross section.

During the present work an accurate track count was made. Events and tracks were classified with identical criteria. Incidence angles and fiducial region were carefully controlled. This allowed us to determine the total cross section for the  $\pi^-+p$  events previously analysed in Bologna (4). The cross-section obtained is

$$\sigma_{el} = (26.7 \pm 1.9) \text{ mb.}$$

This result confirms the assumption that the peak at 890 MeV in the  $\pi^-+p$  total cross section is mainly due to elastic scattering. The inelastic cross section is the same (inside errors) at 915 and 960 MeV while the elastic part is substantially higher at 915 MeV.

## APPENDIX II

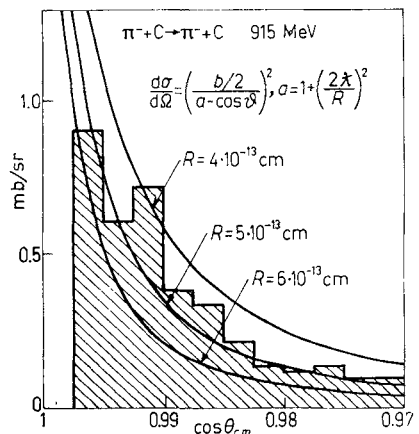
### Another diffraction scattering analysis.

We performed on our carbon data the phenomenological analysis proposed by ITO *et al.* (11) finding an optical radius

$$R = (4.6 \pm 0.3) \cdot 10^{-13} \text{ cm.}$$

The curves illustrating this analysis are shown in Fig. 7.

Fig. 7. - Diffraction scattering analysis following the method of ITO *et al.* (11).



(11) D. ITO, T. KOBAYASHI, M. YAMAZAKI and S. MINAMI: *Progr. Theor. Phys.*, **18**, 264 (1957).

The method of ITO *et al.* differs from the method used in the present work; it assumes a different form of the nuclear potential and uses a different mathematical approximation.

The r.m.s. radius for a uniform sphere of radius  $R$  would be

$$a = (3.55 \pm 0.23) \cdot 10^{-13} \text{ cm.}$$

However, this radius cannot be compared with our values because the mathematical simplifications introduced by ITO *et al.* are such that the relation  $R = \sqrt{\frac{3}{5}} \cdot a$  corresponding to a sphere of uniform density is not correct.

---

#### RIASSUNTO

Sono state studiate le interazioni dei mesoni  $\pi^-$  con nuclei di carbonio, mediante una camera a bolle a propano. Si è trovata una sezione d'urto su carbonio di  $(383 \pm 20)$  mb di cui  $(89 \pm 12)$  mb corrispondono a scattering elastico. Si dà una descrizione dettagliata degli eventi nei quali un mesone  $\pi^-$  viene riemesso. La distribuzione angolare di diffrazione e la sezione d'urto totale sono state descritte con un modello ottico, usando un potenziale immaginario di tipo gaussiano. Il raggio quadratico medio di questo potenziale è risultato  $3.0 \cdot 10^{-13}$  cm; questo valore è considerevolmente maggiore di quello ottenuto per la distribuzione della carica elettrica.